STUDIES OF DROPLET BURNING AND EXTINCTION

F.A. Williams
Department of Applied Mechanics and Engineering Sciences
University of California, San Diego
La Jolla, California 92093-0310

N93-20212

Introduction

A project on droplet combustion, pursued jointly with F.L. Dryer of Princeton University, has now been in progress for many years. The project involves experiments on the burning of single droplets in various atmospheres, mainly at normal atmospheric pressure and below, performed in drop towers (e.g., ref. 1) and designed to be performed aboard space-based platforms such as the Space Shuttle or the Space Station. It also involves numerical computations on droplet burning, performed mainly at Princeton, and asymptotic analyses of droplet burning, performed mainly at UCSD. The focus of the studies rests primarily on time-dependent droplet-burning characteristics and on extinction phenomena.

The presentation to be given here concerns the recent research on application of asymptotic methods to investigation of the flame structure and extinction of hydrocarbon droplets. These theoretical studies are investigating the extent to which combustion of higher hydrocarbons – heptane, in particular – can be described by four-step reduced chemistry of the kind that has achieved a good degree of success for methane flames. The studies (refs. 2, 3, and 4) have progressed to a point at which a number of definite conclusions can now be stated. These conclusions and the reasoning that led to them are outlined here.

Asymptotic Descriptions of Diffusion Flames

A mixture fraction Z (ref. 5), defined to be zero in the oxidizer and unity in the fuel, serves as an attractive independent variable for analyses of diffusion-flame structures because its adoption enables the problem to be formulated in a universal manner that does not depend on the specific geometrical configuration. However, a unique Z exists only if all relevant Lewis numbers are unity. It has been argued (ref. 3) that for droplet burning, in the transport zones away from the stoichiometric mixture fraction Z_c, Lewis numbers of unity are reasonable approximations, mainly because those for oxygen and products in the outer zone are close enough to unity, while in the fuel zone only the fuel specific heat is relevant (since no other species are transported there), and this is large enough to counteract the small fuel diffusion coefficient, again giving the Lewis number close to unity. It is important to account for Lewis numbers different from unity in the thin reaction zone centered at $Z = Z_c$, but this can be done without difficulty and without affecting the definition of Z, so long as this zone is thin in the mixture-fraction coordinate. Thus, the droplet-burning problem is formulated in terms of the mixture fraction (ref. 2, 3, and 4).

In the mixture-fraction formulation, the simplest asymptotic description is the Burke-Schumann reaction-sheet structure, shown by the straight lines labeled "equilibrium" in figure 1. This limit corresponds to an infinite Damköhler number for one-step, irreversible chemistry and provides the outer, transport-zone solutions to which the reaction-zone solutions are matched. Figure 1 illustrates that in the reaction zone there is a one-parameter family of solutions, the parameter being χ_c, the value at stoichiometry of the scalar dissipation rate

$$\chi = 2D \mid \nabla Z \mid^2, \tag{1}$$

where D is the (local, variable, common) diffusion coefficient of the outer solutions. As χ_c increases, the peak temperature decreases, and eventually an abrupt extinction is approached, at a critical value of χ_c. Figure 1 illustrates this qualitatively on the basis of activation-energy asymptotics (AEA); after extinction the solution is the frozen one given by the dashed lines.

When the mixture-fraction formulation is employed, the distinction between different geometrical configurations arises only through the expression for the scalar dissipation, χ. For a stagnant mixing layer of thickness, l

$$\chi = 2D/l, \tag{2}$$

while for constant-density counterflow mixing with a normal-component strain rate K_O in the oxidizer stream

$$\chi = (K_O/\pi)/\exp\left\{2\left[\mathrm{erfc}^{-1}(2Z_c)\right]^2\right\} \tag{3}$$

in which erfc^{-1} denotes the inverse (not the reciprocal) of the complementary error function. It has recently been shown (ref. 6) that for small Z_c, the usual case encountered in practice, variable-density effects can be included reasonably by placing on the right-hand side of equation (3) the additional factor

$$f = \left[3(\sqrt{\rho_O/\rho_c} + 1)^2\right] \Big/ \left[4(2\sqrt{\rho_O/\rho_c} + 1)\right], \tag{4}$$

where ρ_O is the density of the oxidizing stream and ρ_c that at the stoichiometric flame sheet. For droplet burning (ref. 2) it is found that

$$\chi = \frac{8D}{d_l^2}\left\{\frac{[ln(1-Z)]^2\,(1-Z)}{ln(1+B)}\right\}^2 \tag{5}$$

where d_l is the droplet diameter, and B is the transfer number for the droplet combustion process, given in an approximation of constant specific heat c_p by

$$B = \left\{c_p(T_\infty - T_l) + QY_{O_2\infty}/\left[(3n+1)W_{O_2}/2\right]\right\}/L, \tag{6}$$

where T, W, and Y denote temperature, molecular weight, and mass fraction, the subscript ∞ identifies the ambient atmosphere, L is the energy required to vaporize a unit mass of fuel, Q stands for the heat released per mole of gaseous fuel in combustion, and n represents the number of carbon atoms in the alkane. By use of equation (5) at $Z = Z_c$, the droplet diameter at extinction d_{le}, can be obtained from χ_{ce}, the value of χ_c at extinction, which has been calculated without reference to the specific geometrical configuration.

Figure 2 illustrates how figure 1 is modified by reduced chemistry. This figure pertains to a two-step approximation in which the reaction zone is split into two parts, a fuel-consumption zone and an oxidizer-consumption zone. The asymptotic analyses have addressed flame structures in two-step, three-step, and four-step approximations. Qualitative illustrations of resulting concentration and temperature profiles in physical space are shown in figure 3, in which C_2H_2 is one representative of numerous intermediate fuel species.

Reduced Chemistry

Systematic reductions to four-step mechanisms for alkanes result in the reduced chemistry

$$\begin{aligned}C_nH_{2n+2} + \gamma H + \left[\beta - (n + 1 + \frac{1}{2}\gamma)\right] H_2O + \Big\{ n - \frac{1}{2}\alpha \\ -\frac{1}{2}\left[\beta - (n+1+\frac{1}{2}\gamma)\right]\Big\} O_2 \rightarrow \alpha CO + \beta H_2 + (n-\alpha)CO_2,\end{aligned} \tag{7}$$

$$CO + H_2O \rightleftharpoons CO_2 + H_2, \tag{8}$$

$$2H + M \rightarrow H_2 + M, \tag{9}$$

$$O_2 + 3H_2 \rightleftharpoons 2H + 2H_2O. \tag{10}$$

Equations (7), (8), (9), and (10) describe the fuel-consumption, water-gas shift (or CO-consumption), radical-recombination, and oxygen-consumption (radical-production) steps, respectively, and they proceed mainly at the rates of the elementary steps

$$C_nH_{2n+2} + H \rightarrow C_nH_{2n+1} + H_2, \tag{11}$$

$$CO + OH \rightleftharpoons CO_2 + H, \tag{12}$$

$$H + O_2 + M \rightarrow HO_2 + M, \tag{13}$$

and

$$H + O_2 \rightleftharpoons OH + O, \tag{14}$$

respectively. The values of the constants α, β, and γ in equation (7) depend on the chemical-kinetic description of the fuel chemistry. Studies (refs. 3 and 4) have shown that theoretical predictions are especially sensitive to the value of γ, the number of radicals destroyed for each fuel molecule that is consumed. It may be expected that the larger γ is, the lower will be the radical concentration and the less robust the flame.

For methane (n = 1), the summation

$$\begin{array}{rcl}
CH_4 + H & \rightarrow & CH_3 + H_2 \\
CH_3 + O & \rightarrow & CH_2O + H \\
CH_2O + H & \rightarrow & CHO + H_2 \\
CHO + M & \rightarrow & CO + H + M \\
H + OH & \rightarrow & O + H_2 \\
H + H_2O & \rightarrow & OH + H_2 \\
\hline
CH_4 + 2H + H_2O & \rightarrow & CO + 4H_2
\end{array}$$

with the steps dictated by the need to cancel all steady-state species through their fastest reactions results in $\alpha = 1, \beta = 4$, and $\gamma = 2$. Even excluding the second of these steps by assuming (erroneously) that $2CH_3 + M \rightarrow C_2H_6 + M$ is very fast and that ethane chemistry therefore controls the fuel consumption gives only $\alpha = \frac{1}{2}, \beta = 3$, and $\gamma = 1$, that is, the number of radicals consumed is decreased by just a factor of two. Consequently there is relatively little significant uncertainty in step (7) for methane. However, for a larger alkane, such as heptane, there is a large difference, depending on whether the fuel chemistry follows a propene path after step (11), namely,

$$C_7H_{15} \rightarrow CH_3 + 2C_3H_6 \tag{15}$$

(overall), as proposed by Warnatz, or an ethene path,

$$C_7H_{15} \rightarrow CH_3 + 3C_2H_4 \tag{16}$$

(overall) as favored by Dryer. The propene path gives $\alpha = 7$, $\beta = 20$, and $\gamma = 10$, while the ethene path gives $\alpha = 4$, $\beta = 13$, and $\gamma = 2$, a factor of five difference in the number of radicals consumed. This large factor turns out to have a large influence on the scalar dissipation at extinction because the much greater extent of consumption of radicals by fuel in the propene path leads to extinction much earlier. Since uncertainties in the detailed fuel chemistry of higher hydrocarbons do not enable a selection to be made between the propene and ethene paths, for example, at present, it is concluded that further study of elementary steps and mechanisms in alkane fuel chemistry is needed.

In the present work (ref. 4) experimental results on extinction of burning heptane pools were employed along with the asymptotic theory for the four-step description to infer what value of γ is needed to best fit the data. In this manner, it was found that $\gamma = 13$ is close to the optimum selection. This suggests that revisions in equations (15) or (16) or in the propene and ethene consumption mechanisms are needed if agreement with extinction experiments is to be achieved.

Computations were made not only with the four-step mechanism but also with a three-step mechanism, obtained from the four-step description by putting the H atom in steady state, and with a two-step mechanism, obtained from the three-step description by imposing partial equilibrium on step (8). There were large differences in the resulting predictions of heptane flame structures and extinction, much larger than for methane. For example, differences in the scalar dissipation at extinction exceeded a factor of ten, in contrast to being less than a factor of two for methane. It is concluded that the higher hydrocarbons are more sensitive to the kinetic descriptions and that therefore experiments on flame structures and extinction for these fuels may provide information of greater relevance to the chemical kinetics.

Flame Structure and Extinction

In the two-step approximation, the structure is as illustrated in figure 2, with the fuel-consumption zone thin compared with the oxygen-consumption zone, which in turn occupies an asymptotically small range of Z. In the three-step approximation, nonequilibrium of step (8) occurs in a portion of the oxygen-consumption zone adjacent to the fuel-consumption zone, provided that the Damköhler number for this step is large enough, which it is for the propene path but not for the ethene path. If the ethene path without modification is correct (which seems quite unlikely), then an alternative analysis, paralleling that of Bui-Pham, Seshadri, and Williams for the premixed methane flame with slow CO oxidation, will be needed, but it does not appear that the correct fuel chemistry for alkane diffusion flames will require this. In the four-step approximation, the thin fuel-consumption zone itself has substructure. There are two limiting behaviors of this substructure, as illustrated in figures 4 and 5. When H has a strong tendency to achieve steady state, as was found for methane, there is a thin radical-consumption layer within the fuel-consumption layer, as illustrated in figure 4, where the nondimensional thickness of the fuel-consumption layer is δ, and the parameter μ, (ref. 4) involving ratios of reaction rates in the rate-ratio asymptotic analysis (RRA) is large. When this tendency is weak (μ small), the situation illustrated in figure 5 occurs, in which there is a diffusion flame between radicals and fuel within this inner layer – a diffusion flame within the diffusion flame. The results (ref. 4) show heptane to lie strongly in this last regime ($\mu \rightarrow 0$).

Predictions of the location Z_0 and outer-solution temperature T^0 of the inner fuel-consumption zone are of interest. For heptane, contrary to the relative location illustrated in figure 2, the two-step and three-step descriptions give Z_0 on the oxidizer side of Z_c for most values of χ_c, in particular at extinction. This disagrees with experiment and also with the predictions of the four-step mechanism, which place Z_0 on the fuel side, as illustrated in figure 2, even at extinction. The temperature T^0 of this fuel-consumption zone also is more realistic with the four-step mechanism, as illustrated in figure 6. Thus, in every respect, the four-step description is much better than simpler descriptions for higher hydrocarbons.

From χ_{ce}, equation (5) is used to calculate extinction diameters. Results are shown in figures 7 and 8. Figure 7, for the propene route, clearly shows the large differences obtained with different degrees of reduction of the chemistry. The most reasonable values probably are close to the two-step prediction, fortuitously through cancellations of errors, but until heptane droplet extinction is observed experimentally, this conclusion is not certain. If the four-step predictions in figure 7 are correct, then it is unlikely that droplet extinction can be observed experimentally, because the droplets will become too small. If $\gamma = 13$ in equation (7), then the four-step predictions fall much closer to those shown for the two-step predictions. Comparison of the three-step results shown in figure 8 for the propene and ethene routes shows the extremely large difference in extinction diameters for these two descriptions ($\gamma = 10$ versus $\gamma = 2$); calculations with two-step and four-step chemistry for the ethene route gave essentially zero extinction diameters. It seems likely that many more than two radicals are destroyed for each heptane molecule consumed, but further chemical studies are needed to determine how many.

Future Plans

It is planned to investigate the fuel chemistry further, in an effort to determine better the values of the parameters α, β, and γ. It is also planned to initiate similar asymptotic analyses for alcohol fuel droplets. Finally, microgravity experiments on alkane droplet extinction in different atmospheres are planned, to test predictions.

References

1. Choi, M.Y., Dryer, F.L., Card, J.M., Williams, F.A., Haggard, J.B., Jr., and Borowski, B.A., "Microgravity Combustion of Isolated n-Decane and n-Heptane Droplets," AIAA Paper No. 92-242, January, 1992.

2. Card, J.M. and Williams, F.A., "Asymptotic Analysis of the Structure and Extinction of Spherically Symmetrical n-Heptane Diffusion Flames," Combustion Science and Technology 84 (1992) 91-120.

3. Card, J.M. and Williams, F.A., "Asymptotic Analysis with Reduced Chemistry for the Burning of n-Heptane Droplets," Combustion and Flame, to appear, 1992.

4. Card, J.M., "Asymptotic Analysis for the Burning of n-Heptane Droplets using a Four-Step Reduced Mechanism," Combustion and Flame, submitted, 1992.

5. Williams, F.A., "Combustion Theory," Addison-Wesley, Menlo Park, CA, 1985.

6. Kim, J.S. and Williams, F.A., "Structures of Flow and Mixture-Fraction Fields for Counterflow Diffusion Flames with Small Stoichiometric Mixture Fractions," Combustion Science and Technology, submitted, 1992.

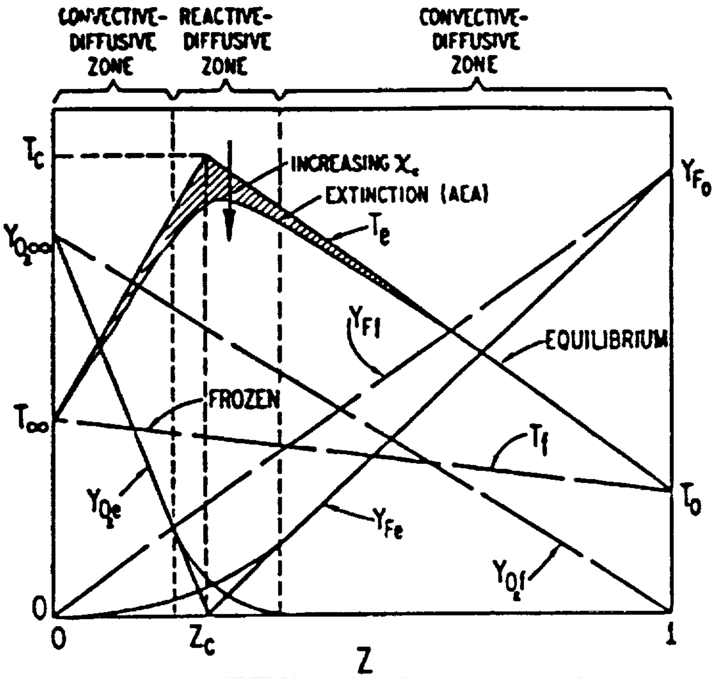

Figure 1.– Schematic diagram of the flame structure in the mixture-fraction coordinate for one-step empirical Arrhenius chemistry, showing fuel (F), oxygen (O_2), and temperature profiles.

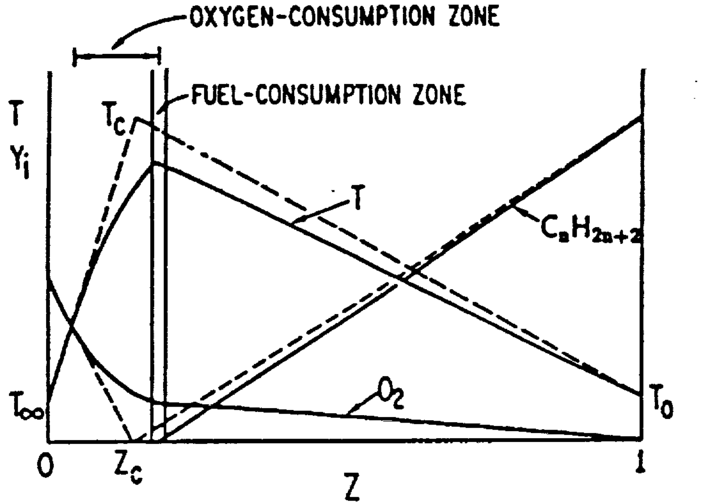

Figure 2.– Schematic diagram of the flame structure in the mixture-fraction coordinate for two-step reduced chemistry.

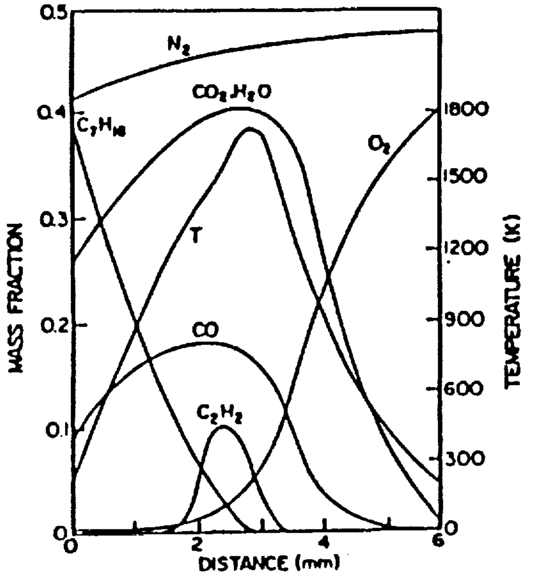

Figure 3.– Schematic illustration of implications of theory concerning heptane flame structure in physical coordinates.

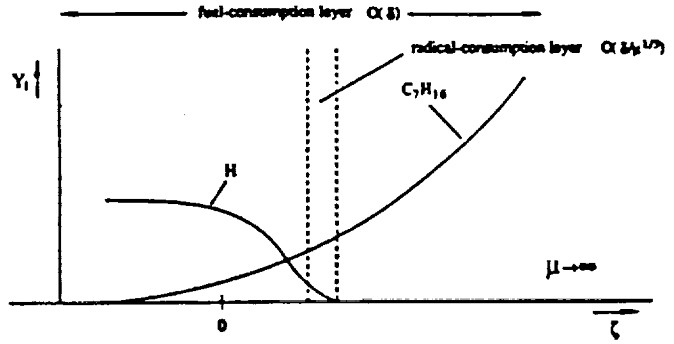

Figure 4.– Schematic illustration of inner-layer structure when there is a strong tendency for H to be in steady state.

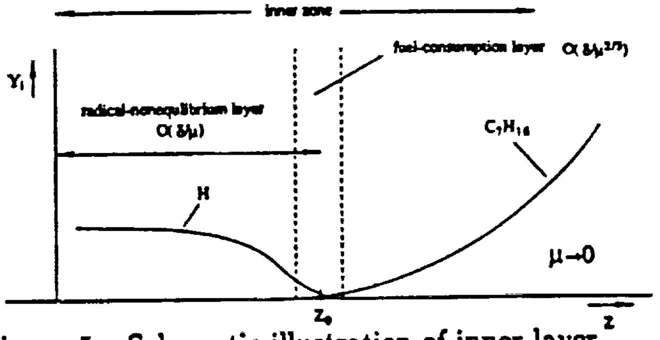

Figure 5.– Schematic illustration of inner-layer structure when there is a weak tendency for H to be in steady state.

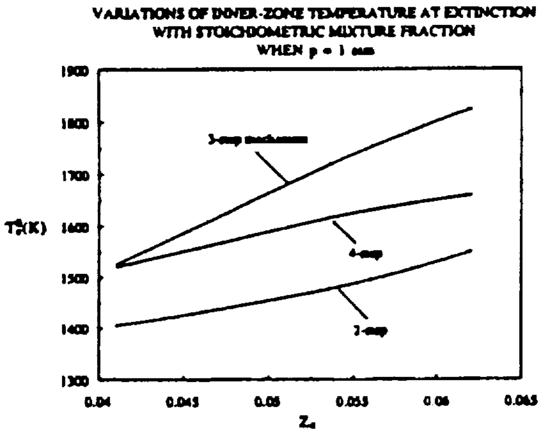

Figure 6.– Dependence of the inner-zone temperature at extinction on the stoichiometric mixture fraction (varied by dilution) for the propene path at normal atmospheric pressure and temperature.

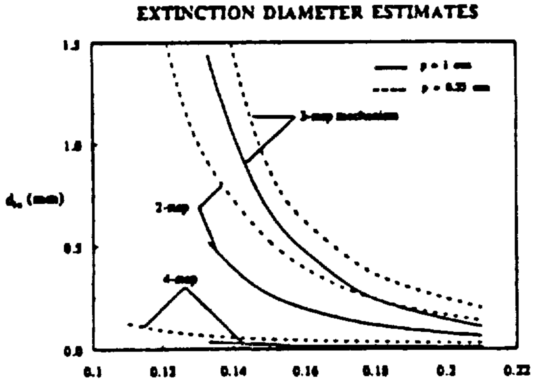

Figure 7.– Predicted dependence of the heptane extinction diameter on the oxygen mole fraction in the ambient gas for the propene path.

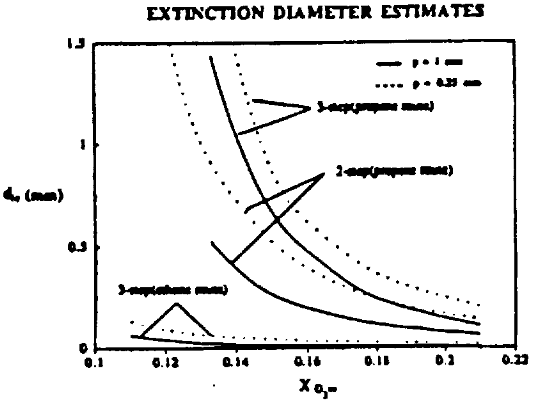

Figure 8.– Predicted dependence of the heptane extinction diameter on the oxygen mole fraction in the ambient gas for both propene and ethene routes.

COMMENTS

Question (Ray Edelman, Rockwell International): I would expect burning rate and extinction, in particular, would depend strongly on soot formation and the attendant radiation loss on reducing temperature. This might be enhanced at high pressures. Could you comment on what your data shows and how you reconcile this with your analyses? Do competing effects balance this with enhanced kinetics at increasing pressure?

Answer: Our studies are at normal atmospheric pressures and at reduced pressures, not at high pressures. For our small single droplets under these conditions, radiant transfer associated with soot formation probably is negligible. At high pressures it will become more important, but temperature reduction through radiant energy loss still could be a perturbation because of the small size.